

# Weierstraß-Institut für Angewandte Analysis und Stochastik

im Forschungsverbund Berlin e.V.

Preprint

ISSN 0946 – 8633

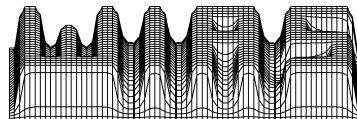
## Macroscopic modeling of porous and granular materials - microstructure, thermodynamics and some boundary-initial value problems

Krzysztof Wilmański

submitted: 8th July 2003

Weierstrass Institute  
for Applied Analysis  
and Stochastics  
Mohrenstraße 39  
10117 Berlin  
Germany  
E-Mail: [wilmansk@wias-berlin.de](mailto:wilmansk@wias-berlin.de)

No. 858  
Berlin 2003



---

2000 *Mathematics Subject Classification.* 35L50, 74J15, 80A17, 74A20, 74F10.

*Key words and phrases.* Thermodynamics, Biot's model, poroelastic materials, acoustic waves, surface waves.

Edited by  
Weierstraß-Institut für Angewandte Analysis und Stochastik (WIAS)  
Mohrenstraße 39  
D — 10117 Berlin  
Germany

Fax: + 49 30 2044975  
E-Mail: [preprint@wias-berlin.de](mailto:preprint@wias-berlin.de)  
World Wide Web: <http://www.wias-berlin.de/>

## Abstract

This work contains the material presented in the key lecture during the Congress Cancam 2003 (Calgary, Canada). It contains a review of the recent development of thermodynamic modeling of porous and granular materials. We present briefly main features of the thermodynamic construction of a non-linear poroelastic model but the emphasis is put on the analysis of a linear two-component model. In particular we indicate similarities and differences of the thermodynamic model with the classical Biot's model of porous materials. We analyze jacketed and unjacketed Gedankenexperiments which provide a micro-macrotransition procedure for compressibilities. This gives rise to Gassmann-like relations which are incorporated in wave analysis. An acoustic waves analysis is presented in some details. In particular we show the construction of bulk monochromatic waves as well as some surface waves and indicate their practical applications in testing of soils.

## 1 Introduction

Porous materials appear in nature so often that we tend to overlook them. Soils and rocks, biological tissues, wood and paper, ceramics like bricks or microfilters, etc. All of them are characterized by a microstructure which consists of a solid frame – a skeleton, channels which are voids in the solid frame (pores), and fluids filling channels. The most characteristic feature of mechanical processes in such materials is the relative motion of fluid components with respect to the skeleton, i.e. there appears a *diffusion*.

Macroscopic modeling of such media is usually based on a theory of mixtures. Due to the presence of a solid component such mixtures are called *immiscible*.

From the point of view of technical applications of such models one can distinguish two very simple classes of models:

- 1) a solid skeleton is described as it was a normal solid whose effective (macroscopic) parameters are dependent on the porosity (volume fraction of voids), and a motion of a fluid is described by an additional field equation – usually a parabolic partial differential equation (Darcy model),
- 2) a solid skeleton is considered to be rigid (not deformable) and solely an effective motion of a mixture of fluids is described by a classical theory of miscible fluids.

The first class appears in particular in applications to soil mechanics and the model of consolidation introduced by Terzaghi is the most prominent example of such a

model. To the same class belongs the model proposed by Kolymbas for plastic deformations of rocks (hypoplasticity).

The second class of models is frequently used to describe flows of ground water (e.g. Non-aqueous Phase Liquid – NAPL), sedimentation, motion of pollutants, etc.

In the general case one can expect couplings between deformations of the skeleton and motions of fluid components. For instance, deformable solid and fluid components must be accounted for in the wave analysis in geophysical problems. Consequently the *thermodynamic modeling of immiscible mixture* seems to be an appropriate macroscopic way to describe such media.

The first linear model proposed for a two-component poroelastic fully saturated material was published in 1941 by M. A. Biot [1]. This model predicts correctly many properties of linear acoustic waves in porous materials. For instance it yields the existence of an additional mode of propagation of bulk waves – the so-called P2- (slow, Biot’s) wave. Generalizations of the model on viscoelastic materials and viscous fluids are still commonly and successfully used in geotechnics.

The fully nonlinear multicomponent thermodynamical model of immiscible mixtures has been developed by R. M. Bowen (e.g. see his contribution to the book [2]). The model which we present in this lecture belongs to the same class even though there are some differences (e.g. the consistent Lagrangian description, the form of porosity balance equation, etc.). Basic features of the model used in the present contribution can be found in my book [3].

## 2 Microstructure

In contrast to miscible mixtures porous and granular materials possess microstructure which goes beyond different mass densities (or concentrations) and different velocities of components. The most important additional microstructural feature is the porosity. It may be related to interconnected voids or to cavities without any connection with channels. These channels possess an additional property essential for diffusive motions – tortuosity. This quantity measures the ratio of the real length of channels to a characteristic macroscopic length. In addition some fluid components may exchange the mass with the skeleton due to freezing, adsorption, evaporation and cavitation, etc. All these microstructural variables require additional equations describing their temporal and spacial variations.

The full thermodynamic description of all those microstructural properties is not yet available. Existing models account for changes of porosity, for mass exchange due to chemical reactions and some phase transformations. However, very little has been done for such processes as evaporation leading to unsaturated media, or adsorption processes for high concentrations of adsorbate.

Further we present only a few chosen features of thermodynamic modeling based on general principles of evaluation of the second law of thermodynamics (e.g. see [4]).

### 3 Multicomponent continuous models

The aim of macroscopic thermodynamic modeling of porous and granular materials is to find field equations for the following quantities (fields)

- $\rho_t^S$  - current partial mass density of the skeleton,
- $\rho_t^\alpha$  - current partial mass densities of fluid components,  $\alpha = 1, \dots, A$ ,
- $\mathbf{F}^S$  - deformation gradient of the skeleton,
- $\mathbf{v}^S$  - velocity of the skeleton,
- $\mathbf{v}^\alpha$  - velocities of fluid components,
- $\theta^S$  - temperature of the skeleton,
- $\theta^\alpha$  - partial temperatures of fluid components,
- $\nu^m$  - internal variables (porosity, tortuosity, extents of chemical reactions, phase fractions, plastic deformations, number of occupied sites, etc.),  $m = 1, \dots, M$ .

In the construction of field equations for macroscopic fields one usually relies on partial balance equations of mass, momentum, and energy. For the internal variables additional equations are required and these follow from particular physical considerations. These are, for example, a balance equation of porosity, an equation for equilibrated forces, proposed by Goodman and Cowin to describe microinertia, an evolution equation for occupied sites in adsorption processes, proposed by Langmuir, an evolution equation for stresses in hypoplasticity, proposed by Kolymbas, etc.

Construction of these additional equations may be supported by some microscopic considerations such as a kinetic theory of granular gases, or properties of simple tests and a micro-macrotransition for homogeneous granular microstructures. We present further an example of such a transition.

Let us consider a simple example of such a model – a linear two-component isothermal medium. In the Eulerian description the fundamental balance laws have the form

1) partial mass balance equations

$$\frac{\partial \rho_t^S}{\partial t} + \operatorname{div}(\rho_t^S \mathbf{v}^S) = \hat{\rho}^S, \quad \frac{\partial \rho_t^F}{\partial t} + \operatorname{div}(\rho_t^F \mathbf{v}^F) = -\hat{\rho}^S, \quad (1)$$

2) partial momentum balance equations

$$\frac{\partial \rho_t^S \mathbf{v}^S}{\partial t} + \operatorname{div}(\rho_t^S \mathbf{v}^S \otimes \mathbf{v}^S - \mathbf{T}^S) = \hat{\mathbf{p}}, \quad \frac{\partial \rho_t^F \mathbf{v}^F}{\partial t} + \operatorname{div}(\rho_t^F \mathbf{v}^F \otimes \mathbf{v}^F - \mathbf{T}^F) = -\hat{\mathbf{p}}, \quad (2)$$

3) balance equation for porosity

$$\frac{\partial n J^{S-1}}{\partial t} + \operatorname{div} (n \mathbf{v}^S + \Phi (\mathbf{v}^F - \mathbf{v}^S)) = (\hat{n} + \delta \frac{\partial J^S}{\partial t}) J^{S-1}, \quad (3)$$

$$J^S := 1 + e, \quad e := tr \mathbf{e}^S,$$

4) integrability conditions for small deformations

$$\frac{\partial \mathbf{e}^S}{\partial t} = \operatorname{grad} \mathbf{v}^S, \quad \operatorname{grad} \mathbf{e}^S = (\operatorname{grad} \mathbf{e}^S)^{23}, \quad \mathbf{e}^S := \frac{1}{2} (\mathbf{1} - \mathbf{F}^{S-1} \mathbf{F}^{S-T}), \quad (4)$$

where  $\rho_t^S, \rho_t^F$  are current mass densities of skeleton and fluid, respectively,  $\mathbf{v}^S, \mathbf{v}^F$  are velocities of components (their local difference defines the diffusion velocity),  $\mathbf{T}^S, \mathbf{T}^F$  are Cauchy partial stress tensors for both components,  $\mathbf{e}^S$  is the Almansi-Hamel tensor of small deformations of skeleton,  $n$  is the porosity,  $\hat{\rho}^S, \hat{\mathbf{p}}, \hat{n}$  are sources of mass, momentum, and porosity, respectively. The first one describes the rate of exchange of mass between components (e.g. melting rate or adsorption rate), the second one describes the so-called diffusive force (an internal friction due to the relative motion of components), and the third one describes relaxation properties of porosity.  $\Phi$  and  $\delta$  are material parameters.

In order to transform the above equations into field equations one has to specify the dependence of constitutive quantities

$$\{\hat{\rho}^S, \hat{\mathbf{p}}, \mathbf{T}^S, \mathbf{T}^F, \Phi, \delta, \hat{n}\} \quad (5)$$

on constitutive variables. These are the so-called *constitutive relations*.

For poroelastic materials without mass exchange these variables are as follows

$$\{\mathbf{e}^S, \rho_t^F, \mathbf{v}^F - \mathbf{v}^S, n\}. \quad (6)$$

For other materials such as elastoplastic skeleton or exchange of mass between components this set must be chosen accordingly.

## 4 Thermodynamics and thermodynamic models

Once the set of governing equations has been chosen and constitutive relations were specified we have to check if some fundamental laws of macroscopic models are satisfied. They do so automatically if we construct an empirical model based on experimental observations. This is seldom the case and usually we choose constitutive relations in a much more general form than this which we can verify in simple experiments. Then we impose the following conditions:

- Any solution of field equations (i.e. the so-called thermodynamic process) must satisfy the *entropy inequality*. This is the *second law of thermodynamics*. In the particular case of a two-component system the entropy inequality has the form

$$\frac{\partial}{\partial t}(\rho_t^S \eta^S + \rho_t^F \eta^F) + \operatorname{div}(\rho_t^S \eta^S \mathbf{v}^S + \rho_t^F \eta^F \mathbf{v}^F + \mathbf{h}^S + \mathbf{h}^F) \geq 0, \quad (7)$$

where  $\eta^S, \eta^F$  are partial entropy densities, and  $\mathbf{h}^S, \mathbf{h}^F$  – their fluxes. They must depend on chosen constitutive variables.

– All constitutive relations must be invariant with respect to a rigid time dependent motion of the frame (the *material objectivity*).

Exploitation of these conditions yields a number of limitations on constitutive relations (such as the Gibbs equation or Maxwell relations in classical thermostatics). One of them is the so-called *dissipation inequality* which describes a deviation of processes from the thermodynamic equilibrium in which the dissipation is equal to zero.

In the example of the two-component system quoted above the dissipation is as follows

$$D := (\mu^S - \mu^F) \hat{\rho}^S + \hat{\mathbf{p}} \cdot (\mathbf{v}^F - \mathbf{v}^S) + \frac{\partial}{\partial n}(\rho_t^S \psi^S + \rho_t^F \psi^F) \hat{n} \geq 0, \quad (8)$$

where  $\psi^S, \psi^F$  are constitutive functions called Helmholtz *free energy* functions,  $\mu^S, \mu^F$  are *chemical potentials* given by derivatives of free energies with respect to partial mass densities. In a linear model this inequality indicates that the mass source is proportional to the difference of chemical potentials (see, e.g. theories of drying of wood and ceramics), the source of momentum (the diffusive force) is proportional to the diffusive (relative) velocity and that the source of porosity is a linear function of the deviation of porosity from its equilibrium value:  $n - n_E$ .

More general models of elastoplastic porous materials, non-Newtonian fluids etc. require a new thermodynamical analysis. These thermodynamic admissibility conditions have been formulated in the literature only for some particular cases. Many models used in practice are constructed ad hoc and thermodynamics is ignored. One can quote many such models which violate the second law of thermodynamics.

One of the most important thermodynamic problems still open even in its basic principles is the construction of models with different partial temperatures. This seems to have a big practical bearing but it is still unknown how to construct thermal quantities of such models and how to formulate the second law of thermodynamics.

In order to illustrate the role of the second law of thermodynamics in the construction of models we present some details concerning the famous Biot's model of poroelastic materials. Biot constructed a linear two-component model of poroelastic materials described by fields of velocities  $\mathbf{v}^S, \mathbf{v}^F$ , the deformation tensor of the skeleton  $\mathbf{e}^S$  and the so-called increment of fluid content  $\zeta$  related in the following way to the above used variables

$$\zeta = n_0 \left( e - \frac{\rho_0^F - \rho_t^F}{\rho_0^F} \right), \quad e \equiv \operatorname{tr} \mathbf{e}^S, \quad (9)$$

where zero denotes an initial constant value of the quantity. By means of the stress potential the constitutive relations for the bulk stress tensor  $\mathbf{T} := \mathbf{T}^S + \mathbf{T}^F$  and for the pore pressure have been formulated.

It can be shown that such a model may follow from the thermodynamic analysis provided we make the following two assumptions about the model:

- 1) we include a constitutive dependence on the gradient of porosity:  $\text{grad } n$ ,
- 2) we neglect relaxation processes of porosity:  $\hat{n} = 0$ .

If this is the case the constitutive relations

$$\begin{aligned}\mathbf{T} &= \mathbf{T}_0 + (K - \frac{2}{3}\mu^S)e\mathbf{1} + 2\mu^S\mathbf{e}^S - C\zeta\mathbf{1}, \\ \mathbf{T}^F &= -n_0p_f\mathbf{1}, \quad p_f = p_f^0 - Ce + M\zeta - N\frac{n - n_0}{n_0},\end{aligned}\tag{10}$$

where

$$n = n_0(1 + \delta e + \frac{\gamma}{n_0}\zeta), \quad \gamma := \frac{\Phi}{n_0},\tag{11}$$

satisfy both the second law of thermodynamics and the porosity balance equation with  $\hat{n} = 0$ . In these relations  $K, \mu^S, C, M, \delta, \gamma, N$  are material parameters depending on the initial porosity  $n_0$  and  $\mathbf{T}_0, p_f^0$  are the bulk initial stresses and the initial pore pressure, respectively.

It is convenient to write constitutive relations (10) transformed to partial stresses. They have the form

$$\begin{aligned}\mathbf{T}^S &= \mathbf{T}_0^S + \lambda^S e\mathbf{1} + 2\mu^S\mathbf{e}^S + Q\varepsilon\mathbf{1} - N(n - n_0), \\ \mathbf{T}_0^F &= -\left(p_0^F - \rho_0^F\kappa\varepsilon + Qe - N(n - n_0)\right)\mathbf{1}, \quad \varepsilon := \frac{\rho_0^F - \rho_t^F}{\rho_0^F} \equiv e - \frac{\zeta}{n_0},\end{aligned}\tag{12}$$

where material parameters are related in the following way

$$K = \lambda^S + \frac{2}{3}\mu^S + \rho_0^F\kappa + 2Q, \quad C = \frac{1}{n_0}(Q + \rho_0^F\kappa), \quad M = \frac{\rho_0^F\kappa}{n_0}.\tag{13}$$

Relations (10) coincide with Biot's relations provided the constant  $N$  is approximately zero. In order to check this approximation we analyse a set of simple gedankenexperiments.

Before we proceed with this analysis we consider some relations between micro and macro quantities. It is customary to define macroscopic average quantities of porous materials by integrating real microscopic properties of the material over a domain whose volume is small when compared with characteristic macroscopic domains and large compared to such microscopic domains as pores or grains. Such domains are called *Representative Elementary Volumes* (REV) and macroscopic volume averages are defined by integrating over such domains prescribed to macroscopic points  $\mathbf{x}$  of the continuum. Let us introduce a characteristic function  $H(\mathbf{z}, t)$  for the real fluid



component, i.e. a function whose value is one in point  $\mathbf{z}$  occupied by the real fluid at the instant of time  $t$  and zero otherwise. Then we can define the macroscopic (average) current mass density of the fluid  $\rho_t^F(\mathbf{x}, t)$  in a macroscopic point  $\mathbf{x}$  at the instant of time  $t$  by the following relation

$$\rho_t^F(\mathbf{x}, t) = \frac{1}{V} \int_{REV(\mathbf{x}, t)} \rho^{FR}(\mathbf{z}, t) H(\mathbf{z}, t) dV, \quad (14)$$

where  $V$  denotes the volume of REV and  $\rho^{FR}(\mathbf{z}, t)$  is the real (true) mass density of the fluid. Under the assumption of *homogeneous* microstructure this mass density is approximately constant over the domain of REV and we obtain

$$\rho_t^F = n \rho^{FR}, \quad \rho_t^S = (1 - n) \rho^{SR}, \quad n := \frac{1}{V} \int_{REV(\mathbf{x}, t)} H(\mathbf{z}, t) dV, \quad (15)$$

where the second relation for  $\rho_t^S$  follows by a similar argument for the skeleton, and the last relation defines the porosity.

It is convenient to introduce volume changes  $\varepsilon, e, \varepsilon^R, e^R$  in both levels of description by the following definitions

$$\begin{aligned} \rho_t^F &= \frac{\rho_0^F}{1 + \varepsilon}, & \rho_t^S &= \frac{\rho_0^S}{1 + e}, \\ \rho^{FR} &= \frac{\rho_0^{FR}}{1 + \varepsilon^R}, & \rho^{SR} &= \frac{\rho_0^{SR}}{1 + e^R}. \end{aligned} \quad (16)$$

Mass balance equations (without mass exchange!) indicate then

$$\frac{\partial \varepsilon}{\partial t} = \operatorname{div} \mathbf{v}^F, \quad \frac{\partial e}{\partial t} = \operatorname{div} \mathbf{v}^S. \quad (17)$$

Substitution of relations (16) in (15) yields the following geometric compatibility relations for the above described micro-macrotransition

$$e = e^R + \frac{n - n_0}{1 - n_0}, \quad \varepsilon = \varepsilon^R - \frac{n - n_0}{n_0}. \quad (18)$$

Simultaneously we have

$$\zeta = n_0(e - \varepsilon). \quad (19)$$

We are now in the position to consider the above mentioned gedankenexperiments. They have been discussed by Biot and Willis (compare [1]) even though their origin is older. We consider two classes of systems: a jacketed system shown in Fig.1 and an unjacketed system shown in Fig.2.

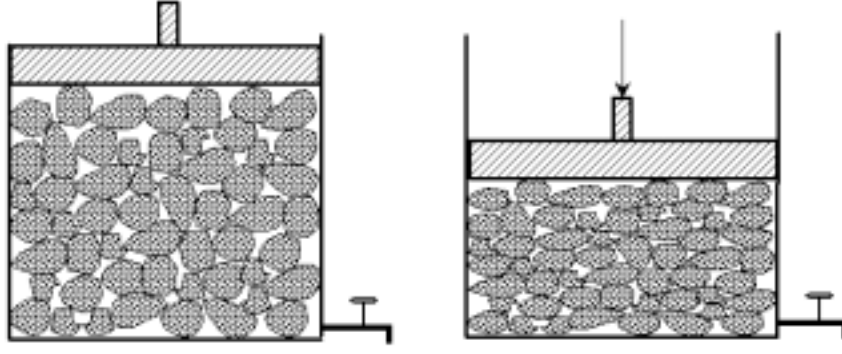


**Figure 1:** *Jacketed Gedankenexperiments*

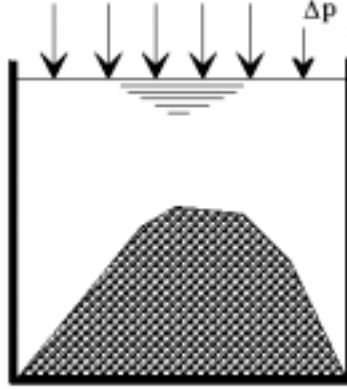


**Figure 2:** *Unjacketed Gedankenexperiment*

In the first case we consider two experiments: undrained when the valve is closed and drained with the open valve. These two experiments are described by the following conditions

$$\zeta = 0 \quad -undrained, \quad p_f - p_f^0 = 0 \quad -drained. \quad (20)$$

For the second,unjacketed system we have the following condition

$$p' = p_f - p_f^0, \quad (21)$$

where  $p'$  is the excess pressure applied to the system.

It can be shown that equilibrium conditions, macroscopic constitutive relations (10) and the microscopic constitutive relations for real pressures in the skeleton and in the fluid

$$p^{SR} - p_0^{SR} = -K_s e^R, \quad p^{FR} - p_0^{FR} = -K_f \varepsilon^R, \quad (22)$$

yield solutions of these three homogeneous problems and, additionally, three compatibility relations between materials parameters. Certainly,  $K_s, K_f$  denote true compressibility moduli of the skeleton and of the fluid respectively.

The above mentioned compatibility relations have the following form

$$\begin{aligned}
0 &= K - K_V + n_0(K_s - K_f) \frac{C - K_f}{K_f - N}, \\
0 &= \frac{K_s}{K_b} \left( n_0 - \frac{C}{M} \right) - \frac{K_s}{K_n} \left( n_0 - \frac{N(K + C)}{K_b M} \right), \\
0 &= K - 2C + M + \frac{MK_b}{K_W} + N \frac{1 - n_0}{n_0} \left( \frac{K}{K_s} \left( 1 - \frac{C}{K} \right) - 1 + \frac{C}{K_W} \right), \\
0 &= K_d - K_b \left( 1 + \frac{NC}{K_b M} \frac{1}{K_n} \right)^{-1},
\end{aligned} \tag{23}$$

where

$$\begin{aligned}
K_V &:= (1 - n_0)K_s + n_0K_f, \quad \frac{1}{K_W} := \frac{1 - n_0}{K_s} + \frac{n_0}{K_f}, \\
K_n &:= K_s \frac{(1 - n_0) \frac{NC}{K_b M} - n_0}{1 - (1 - n_0) \frac{K_s}{K_b}}, \quad K_b := K - \frac{C^2}{M},
\end{aligned} \tag{24}$$

and  $K_d$  denotes the so-called drained compressibility modulus measured in the drained jacketed real experiment.

If we ignore the compatibility relation  $(23)_2$  following from the drained jacketed experiment and assume  $N = 0$  then the above equations lead to the so-called Gassmann relations for macroscopic compressibility parameters (e.g. see [5]). If we do not make this simplification the results for macroscopic parameters differ from those obtained by Gassmann but substantial differences appear primarily in the range of small porosities (see: Fig.3 and Fig.4). In addition it is seen that values of the constant  $N$  are indeed much smaller than values of other material parameters (app. 5-10%).

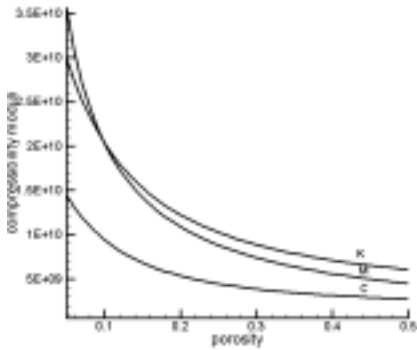


**Figure 3 (left):** Macroscopic material parameters according to classical Gassmann relations with  $N = 0$  and  $K_s = 48 \text{ GPa}$ ,  $K_f = 2.25 \text{ GPa}$

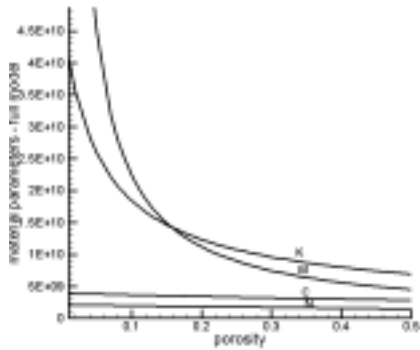


**Figure 4 (right):** Macroscopic material parameters of the model with porosity gradient,  $K_s = 48 \text{ GPa}$ ,  $K_f = 2.25 \text{ GPa}$

In addition solutions for porosity in the above homogeneous experiments give rise to the following relations for material parameters appearing in the relation (11) for porosity

$$\delta = \frac{K_V - K}{n_0(K_s - K_f)}, \quad \gamma = \frac{C - K_f}{K_s - K_f}. \quad (25)$$

These are illustrated in Fig.5 for the same data as before. Clearly an influence of the nonequilibrium (diffusion) processes becomes essential solely in the range of moderate porosities ( $n_0 \sim 0.2$ ).

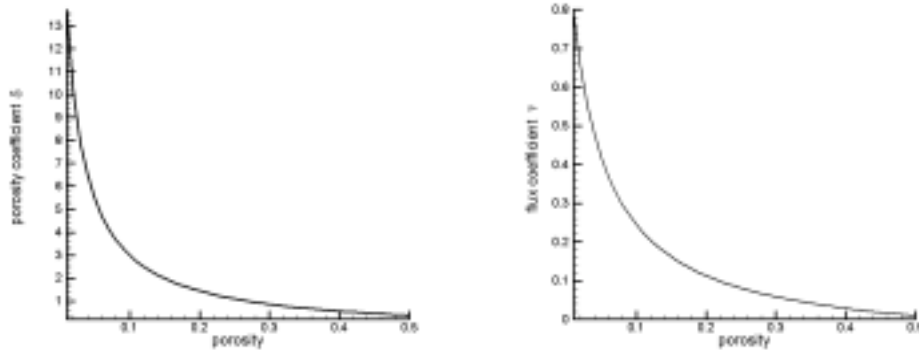


**Figure 5:** Coefficient  $\delta$  (equilibrium, left) and coefficient  $\gamma$  (nonequilibrium, right) of the porosity relation for  $K_s = 48GPa$ ,  $K_f = 2.25GPa$

The dependence of shear modulus  $\mu^S$  on microscopic properties cannot be estimated in this simple matter. There are some attempts to derive this relation from the solution of Hertz contact problem for particular arrangements of granuli but they are not very reliable.

One should stress that, in general, the above linear model does not reflect too well real properties of granular materials due to the lack of dependence on confining pressure (dilatancy problem) and other nonlinear effects. Research in this field is still not very advanced. However the results indicated above are sufficient for the linear wave analysis essential in practical geotechnical testing problems. We present some aspects of these problems further in this lecture.

## 5 Some boundary-initial value problems

### 5.1 Bulk monochromatic waves

As we have mentioned above one of the main reasons for investigating **poroelastic** models is their applicability in the description of acoustic waves of small amplitude. Such waves are a perfect tool for testing morphology (porosity, degree of saturation,

heterogeneity and inclusions, etc.) of soils. Application of surface waves yields even a nondestructive testing particularly desired for economical reasons.

We proceed to present some features of such a wave analysis and we rely on a simple model in which we assume

$$Q := n_0(C - n_0 M) \approx 0, \quad N \approx 0. \quad (26)$$

As indicated above realistic numerical data support this simplification.

We consider two problems: properties of monochromatic bulk waves and properties of surface waves in the low frequency approximation. We conduct the analysis for a chosen real frequency  $\omega$ . This choice indicates that we consider waves initiated on the boundary by a harmonic source. However we consider solely solutions far away from the source (*far field approximation*) in order to avoid solving complicated boundary value problems.

Let us begin with bulk waves in two-component (fully saturated) poroelastic material whose fields have the following form

$$\begin{aligned} \rho_t^F - \rho_0^F &= R^F e^{i(k\mathbf{n} \cdot \mathbf{x} - \omega t)}, & \mathbf{e}^S &= \mathbf{E}^S e^{i(k\mathbf{n} \cdot \mathbf{x} - \omega t)}, \\ \mathbf{v}^F &= \mathbf{V}^F e^{i(k\mathbf{n} \cdot \mathbf{x} - \omega t)}, & \mathbf{v}^S &= \mathbf{V}^S e^{i(k\mathbf{n} \cdot \mathbf{x} - \omega t)}. \end{aligned} \quad (27)$$

In these relations  $\mathbf{n}$  is the unit vector pointing in the direction of propagation,  $k$  is the wave number and it is usually complex,  $\omega$  is the frequency of the wave and it is assumed to be real and given,  $R^F, \mathbf{E}^S, \mathbf{V}^F, \mathbf{V}^S$  are constant amplitudes of the waves. Substitution in field equations yields the following compatibility relations

$$R^F = \frac{k\rho_0^F}{\omega} \mathbf{V}^F \cdot \mathbf{n}, \quad \mathbf{E}^S = -\frac{k}{2\omega} (\mathbf{V}^S \otimes \mathbf{n} + \mathbf{n} \otimes \mathbf{V}^S), \quad (28)$$

$$\left( \omega^2 \mathbf{1} - (c_{P1}^2 - c_S^2) k^2 \mathbf{n} \otimes \mathbf{n} - c_S^2 k^2 \mathbf{1} + i \frac{\pi\omega}{\rho_0^S} \mathbf{1} \right) \mathbf{V}^S - i \frac{\pi\omega}{\rho_0^S} \mathbf{V}^F = 0, \quad (29)$$

$$-i \frac{\pi\omega}{\rho_0^F} \mathbf{V}^S + \left( \omega^2 \mathbf{1} - c_{P2}^2 k^2 \mathbf{n} \otimes \mathbf{n} + i \frac{\pi\omega}{\rho_0^F} \mathbf{1} \right) \mathbf{V}^F = 0,$$

where

$$c_{P1}^2 := \frac{\lambda^S + 2\mu^S}{\rho_0^S}, \quad c_{P2}^2 := \kappa, \quad c_S^2 := \frac{\mu^S}{\rho_0^S}. \quad (30)$$

This is, of course, an eigenvalue problem. We seek its solution separating components of equations (29) in the direction parallel to  $\mathbf{n}$  and perpendicular to  $\mathbf{n}$ .

Let us first take the scalar product of equations (29) with a unit vector perpendicular to  $\mathbf{n}$ . We obtain the set of homogeneous algebraic relations for the components of  $\mathbf{V}^S, \mathbf{V}^F$  perpendicular to  $\mathbf{n}$ , i.e. the second – transversal – case. It follows that we have to satisfy the following *dispersion relation* which is the determinant of the set

$$\omega \left( \frac{\omega^2}{k^2} - c_S^2 \right) + i \frac{\pi}{\rho_0^F} \left( \frac{\rho_0^F + \rho_0^S}{\rho_0^F} \frac{\omega^2}{k^2} - c_S^2 \right) = 0. \quad (31)$$

Consequently we obtain a relation  $k = k(\omega)$  which yields relations for the so-called *phase speed*  $c_{ph} := \omega/Rek$ , and for the *attenuation*  $Imk$  of the so-called S-wave. These are shown in Fig.6 for the following data typical for rocks

$$\begin{aligned} c_{P1} &= 2500 \frac{m}{s}, & c_{P2} &= 1000 \frac{m}{s}, & c_S &= 1500 \frac{m}{s}, \\ \rho_0^F &= 250 \frac{kg}{m^3} \quad (n_0 = 0.25), & \rho_0^S &= 2500 \frac{kg}{m^3}, \\ \pi &= 10^6, 5 \times 10^6, 10^7, 5 \times 10^7, 10^8 \frac{kg}{m^3 s}. \end{aligned} \quad (32)$$

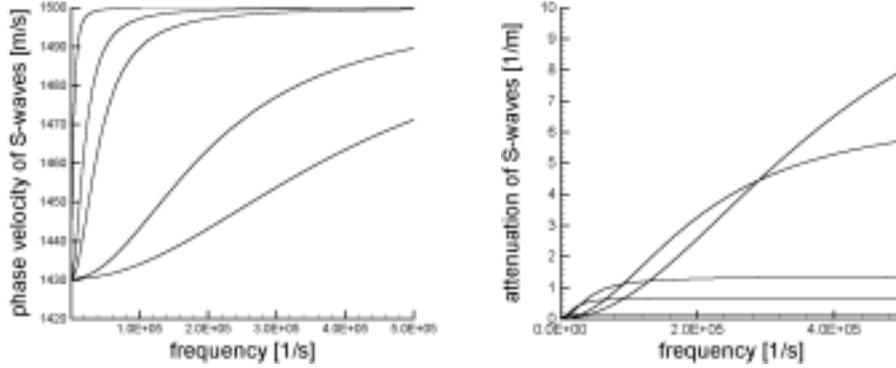


**Figure 6:** Phase speed (left) and attenuation (right) of S-wave.

The upper curve in the vicinity of  $\omega = 0$  corresponds to the lowest value of the permeability coefficient  $\pi$

It is easy to see that the phase speeds in the limits  $\omega \rightarrow 0$  and  $\omega \rightarrow \infty$  are different. They can be easily calculated from the dispersion relation and we obtain

$$\lim_{\omega \rightarrow \infty} c_{ph} = c_S = \sqrt{\frac{\mu^S}{\rho_0^S}}, \quad \lim_{\omega \rightarrow 0} c_{ph} =: c_{oS} = \sqrt{\frac{\mu^S}{\rho_0^S + \rho_0^F}}. \quad (33)$$

The second result – *low frequency limit* – is this which is measured in geotechnical experiments (frequencies 1Hz). The first one appears, for instance, in medical applications (frequencies 1MHz).

Scalar multiplication of equations (29) by the vector  $\mathbf{n}$  yields the eigenvalue problem for longitudinal waves. We obtain the following solution of the dispersion relation

$$\begin{aligned} k^2 &= \frac{1}{2} \left[ \frac{1}{c_{P1}^2} \left( \omega^2 + i \frac{\pi \omega}{\rho_0^S} \right) + \frac{1}{c_{P2}^2} \left( \omega^2 + i \frac{\pi \omega}{\rho_0^F} \right) \pm \sqrt{D} \right], \\ D &:= \left[ \frac{1}{c_{P1}^2} \left( \omega^2 + i \frac{\pi \omega}{\rho_0^S} \right) - \frac{1}{c_{P2}^2} \left( \omega^2 + i \frac{\pi \omega}{\rho_0^F} \right) \right]^2 - \frac{4}{c_{P1}^2 c_{P2}^2} \frac{\pi^2 \omega^2}{\rho_0^S \rho_0^F}. \end{aligned} \quad (34)$$

Hence we have two solutions. The faster one is called the P1-wave, the slower one – P2-wave or the Biot's wave. Their phase speeds and attenuations are illustrated in Fig. 7 and Fig. 8 for the data (32) (e.g. compare [6] and quotations there).

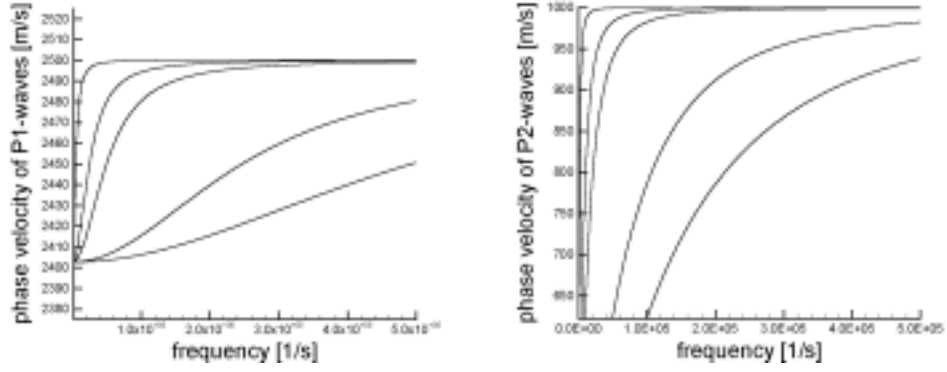


**Figure 7:** *Phase speeds  $c_{ph} = \omega / \text{Re}k$  of P1- (left) and P2-wave (right) for  $\pi$  growing from the upper to lower curve*

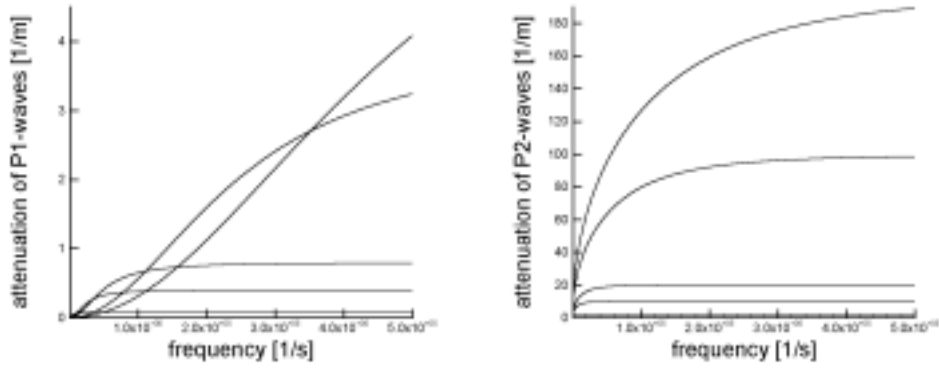


**Figure 8:** *Attenuation  $\text{Im}k$  of P1- (left) and P2-wave (right) for  $\pi$  decaying for large  $\omega$  from the upper to lower curve*

It is seen that the attenuation of P2-waves is two orders of magnitude bigger than the attenuation of P1-waves. This property makes observations of P2-waves in field experiments very difficult indeed. Simultaneously the phase speed of P2-waves goes to zero as the frequency decays to zero. This mode behaves as the system was parabolic in low frequency approximation.

Similarly to shear waves we can construct low and high frequency limits of phase speeds. We obtain after easy calculations

– high frequency limit

$$\lim_{\omega \rightarrow \infty} c_{ph} = \begin{cases} c_{P1} = \sqrt{\frac{\lambda^S + 2\mu^S}{\rho_0^S}} - P1 - wave, \\ c_{P2} = \sqrt{\kappa} - P2 - wave; \end{cases} \quad (35)$$

- low frequency limit

$$\lim_{\omega \rightarrow 0} c_{ph} = \begin{cases} c_{P1} = \sqrt{\frac{\lambda^S + 2\mu^S}{\rho_0^S + \rho_0^F}} - P1 - wave, \\ c_{P2} = 0 - P2 - wave. \end{cases} \quad (36)$$

Bearing the relations from micro-macrotransition as well as an empirical formula for the drained modulus in mind we can construct relations for speeds of propagation  $c_{P1}, c_S, c_{P2}$  as functions of porosity  $n_0$ . This gives rise to the possibility of estimating the porosity of soils *in situ* by measuring the speeds of seismic waves. An example of the scheme of such an experiment is shown in Fig. 9. It shows the standard so-called cross-hole test.

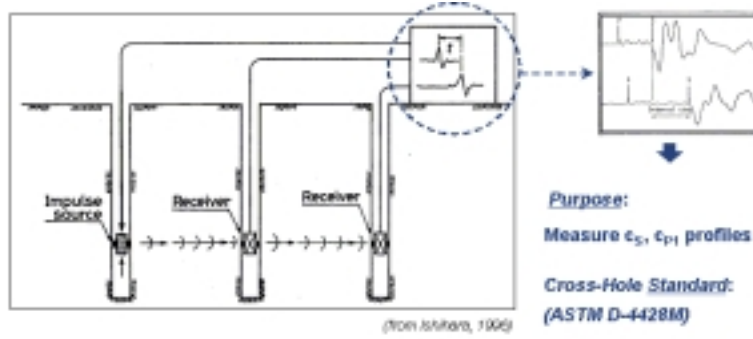


**Figure 9:** *Soil in situ experiments: cross-hole seismic test (example)*

Data from such an experiment obtained in Pisa site has been used by Foti, Lai and Lancellotta [7] to estimate the porosity. They used Gassmann relations and the original Biot's model. The results of this estimate are shown in Fig. 10 in comparison with *in situ* measurements of porosity in Laval and Osterberg tests. Bearing the scattering of such measurements in mind it is clear that the agreement of those results is very good.

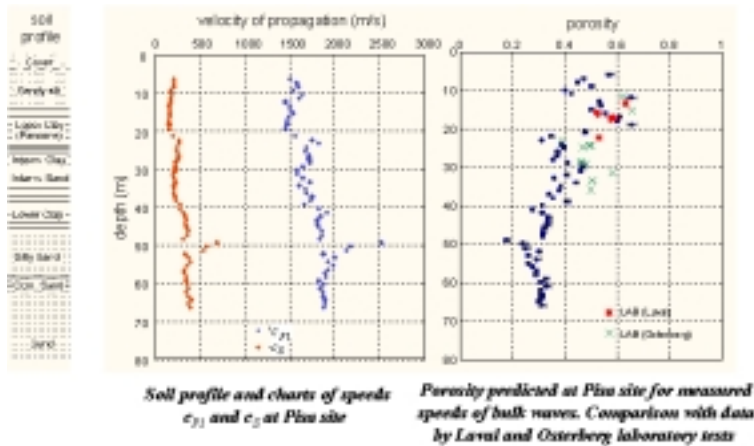


**Figure 10:** *Porosity profile calculated from measurements of speeds  $c_{P1}, c_S$  at Pisa site ([7])*



The above described method of testing soils has one disadvantage. It does not require measurements of porosity on samples taken on the site but it is still destructive and expensive. Namely one has to prepare boreholes for sending and receiving waves. This is not the case if we use surface waves rather than bulk waves. We proceed to present some features of this latter problem.

## 5.2 Surface waves

Surface and interfacial waves are created by a superposition of bulk waves interacting with a boundary. This interaction results from boundary conditions. The best known surface wave is the wave discovered by Rayleigh. It appears on the free boundary of the semiinfinite linear elastic and homogeneous medium. It is schematically shown in Fig. 11.

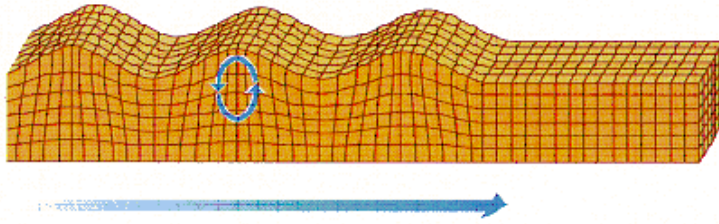


**Figure 11:** *Rayleigh wave - the motion of particles and the direction of propagation*

In this wave motion trajectories of particles are elliptic, particles move in the anticlockwise direction for the wave progressing to the right on the boundary. The amplitude of particles decays exponentially with the depth and this is the reason for calling this motion the surface wave. The speed of propagation  $c_R$  of the classical Rayleigh wave is determined by the following dispersion relation

$$\mathcal{P}_R := \left(2 - \frac{c_R^2}{c_T^2}\right)^2 - 4\sqrt{1 - \frac{c_R^2}{c_T^2}}\sqrt{1 - \frac{c_R^2}{c_L^2}} = 0, \quad c_R < c_T < c_L, \quad (37)$$

where  $c_L, c_T$  are the speeds of the longitudinal and transversal bulk waves. The speed  $c_R$  is independent of frequency (no dispersion!) and there is no attenuation.

The situation becomes much more complicated when a medium is heterogeneous or if it possesses a layered structure. Even in the simplest case of a single elastic layer on a semiinfinite foundation the surface wave possesses infinitely many modes (compare classical Love waves, e.g. [6]). This property of surface waves has a particular bearing in applications to soil mechanics (see: [8]). We do not present any of those problems in the present lecture.

In order to construct surface waves in poroelastic materials we have to formulated boundary conditions.

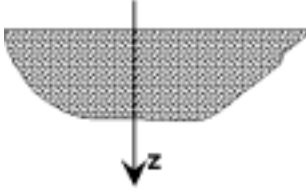


**Figure12** :Boundary of the semiinfinite medium

The boundary of the two-component porous material free of loading and permeable is characterized by the following conditions

$$\begin{aligned}
 T_{xz}|_{z=0} &= T_{xz}^S|_{z=0} = \rho_0^S c_S^2 \left( \frac{\partial u_x^S}{\partial z} + \frac{\partial u_z^S}{\partial x} \right) \Big|_{z=0} = 0, \\
 T_{zz}|_{z=0} &= (T_{zz}^S - p^F)|_{z=0} = \rho_0^S c_{P1}^2 \left( \frac{\partial u_x^S}{\partial x} + \frac{\partial u_z^S}{\partial z} \right) \Big|_{z=0} - \\
 &\quad - 2\rho_0^S c_S^2 \frac{\partial u_x^S}{\partial x} \Big|_{z=0} - c_{P2}^2 (\rho^F - \rho_0^F) \Big|_{z=0} = 0,
 \end{aligned} \tag{38}$$

$$\rho_0^F \frac{\partial}{\partial t} (u_z^F - u_z^S) \Big|_{z=0} - \alpha' \left( \frac{p^{F-}}{n^-} - \frac{p^{F+}}{n^+} \right) = 0, \tag{39}$$

where the axis  $x$  points to the right of the boundary and the axis  $z$  downwards (see: Fig. 12).  $u_x^S, u_z^S$  are components of the vector of displacement of the skeleton and  $u_z^F$  is the component of displacement of the fluid, i.e.

$$\begin{aligned}
 e_{xx}^S &= \frac{\partial u_x^S}{\partial x}, \quad e_{xz}^S = \frac{1}{2} \left( \frac{\partial u_x^S}{\partial z} + \frac{\partial u_z^S}{\partial x} \right), \quad e_{zz}^S = \frac{\partial u_z^S}{\partial z}, \\
 v_x^S &= \frac{\partial u_x^S}{\partial t}, \quad v_z^S = \frac{\partial u_z^S}{\partial t}, \quad v_z^F = \frac{\partial u_z^F}{\partial t}.
 \end{aligned} \tag{40}$$

The condition (39) describes the flow of the fluid through the permeable boundary. The first term is the amount of fluid which flows per unit surface and time through the surface  $z = 0$  and the second term is the driving force of this flow. It is proportional to the difference of true pressures of the fluid  $\frac{p^-}{n^-}, \frac{p^+}{n^+}$  on both sides of the surface and by the material coefficient  $\alpha'$  – surface permeability coefficient. If  $\alpha' = 0$  the boundary is impermeable.

Now we construct the solution of field equations which describes a surface wave. We make the following *ansatz*

$$\begin{aligned}
 u_x^S &= \frac{\partial \varphi^S}{\partial x} + \frac{\partial \psi^S}{\partial z}, \quad u_z^S = \frac{\partial \varphi^S}{\partial z} - \frac{\partial \psi^S}{\partial x}, \\
 u_x^F &= \frac{\partial \varphi^F}{\partial x} + \frac{\partial \psi^F}{\partial z}, \quad u_z^F = \frac{\partial \varphi^F}{\partial z} - \frac{\partial \psi^F}{\partial x},
 \end{aligned} \tag{41}$$

with scalar potentials  $\varphi^S, \varphi^F$ , vector potentials  $\psi^S, \psi^F$  and remaining unknown fields of this two-dimensional problem given by

$$\begin{aligned}\varphi^S &= A^S(z) \mathcal{E}, & \varphi^F &= A^F(z) \mathcal{E}, & \mathcal{E} &:= e^{i(kx - \omega t)}, \\ \psi^S &= B^S(z) \mathcal{E}, & \psi^F &= B^F(z) \mathcal{E}, \\ \rho^S - \rho_0^S &= A_\rho^S(z) \mathcal{E}, & \rho^F - \rho_0^F &= A_\rho^F(z) \mathcal{E}.\end{aligned}\tag{42}$$

Substitution in field equations yields a differential eigenvalue problem with respect to the variable  $z$ . It can be shown [9] that this problem possesses solutions decaying exponentially with  $z$ , i.e. there may exist surface waves. The propagation conditions follow then by means of boundary conditions.

Here we present briefly final results for the impermeable boundary  $\alpha' = 0$  referring to the works [9], [6] where one can find details.

In the range of *high frequencies* the dispersion relation has the following form

$$\mathcal{P}_R \sqrt{1 - \frac{c_{P1}^2}{c_{P2}^2} c_R^2} + \frac{\rho_0^F c_R^4}{\rho_0^S c_S^4} \sqrt{1 - \frac{c_R^2}{c_{P1}^2}} = 0, \tag{43}$$

where  $\mathcal{P}_R$  is the classical Rayleigh dispersion function given by (37) with  $c_T, c_L$  replaced by  $c_S, c_{P1}$ , respectively. Obviously for  $\rho_0^F = 0$  this relation possesses solely the classical solution for the speed of the surface wave  $c_R$ . Otherwise there exist two modes:

- the leaky Rayleigh wave with the speed  $c_R$  smaller than  $c_S$  but larger than  $c_{P2}$ ,
- the so-called Stoneley wave with the speed  $c_R$  smaller than  $c_{P2}$ .

The existence of these two modes is possible because there are three bulk waves which may combine on the boundary to two independent modes of propagation.

In the range of *low frequencies* the speed of the P2-wave becomes zero and we expect only one surface mode to exist. This is indeed the case. The dispersion relation in this approximation has the following form

$$\frac{c_R^2}{c_{P1}^2} \left[ \left( 2 + \frac{\rho_0^F}{\rho_0^S} + 1 \right) \frac{c_R^2}{c_S^2} \right]^2 - 4 \sqrt{1 - \frac{\rho_0^F}{\rho_0^S} + 1} \frac{c_R^2}{c_S^2} \sqrt{1 - \frac{\rho_0^F}{\rho_0^S} + 1} \frac{c_R^2}{\frac{\rho_0^F}{\rho_0^S} \frac{c_{P2}^2}{c_{P1}^2} + 1} \frac{c_R^2}{c_{P1}^2}} = 0. \tag{44}$$

This is approximately the renormalized Rayleigh equation whose solution differs from the classical solution by the following factor

$$c_R \rightarrow \frac{c_{P1}}{c_{oP1}} c_R \equiv \sqrt{\frac{\rho_0^S}{\rho_0^S + \rho_0^F}} c_R. \tag{45}$$

Solely this mode is observed in situ experiments on soils. This Spectral Analysis of Surface Waves (SASW) is usually performed in the so-called multistation arrangement shown in Fig. 13 ([10]).

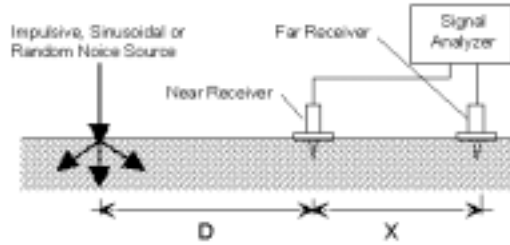


**Figure13 :** *The scheme of multistation configuration for SASW*

In contrast to measurements of bulk waves the analysis of morphology of soils by surface waves is *nondestructive* and, consequently, very advantageous from the economical point of view.

## 6 Final remarks

The overview of the multicomponent modeling of porous and granular materials presented in this lecture makes clear that the subject – even within a linear limit for poroelastic materials – is still in the very early stage of research. Let us list just a few problems which must be investigated in the near future.

- 1) Results for wave analysis should be extended on heterogeneous and stratified media. In particular, existence of additional modes should be included into the linear two-component model of heterogeneous poroelastic media.
- 2) A model of unsaturated poroelastic materials should be developed in which a coupling of phase transformation (evaporation/condensation) with acoustic waves should be incorporated.
- 3) Properties of surface and bulk waves near interfaces between two porous materials should be investigated. The model seems to be already given but the wave analysis is missing.
- 4) A selfconsistent method of micro-macrotransition must be developed in order to avoid large discrepancies between geometrically and dynamically consistent models (Voigt vs. Reuss models, other averaging methods).
- 5) Nonlinear effects such as a dependence on equilibrium porosity or on confining pressure (dilatancy) in granular materials must be included in the wave analysis. This leads to nonlinear waves (e.g. soliton-like or nonlinear surface waves).
- 6) As estimations of porosity are inverse problems they require a mathematical analysis of solutions which is entirely missing.

## References

- [1] I. TOLSTOY; *Acoustics, Elasticity, and Thermodynamics of Porous Media: Twenty-one Papers by M. A. Biot*, Acoustical Society of America, 1991.
- [2] C. A. TRUESDELL, *Rational Thermodynamics*, second edition, Springer, N. Y., 1985.
- [3] K. WILMANSKI; *Thermomechanics of Continua*, Springer, Berlin, 1998.
- [4] I. MÜLLER, *Thermodynamics*, Pitman, Boston, 1985.
- [5] R. D. STOLL; *Sediment Acoustics*, Lecture Notes in Earth Sciences, #26, Springer, New York, 1989.
- [6] K. WILMANSKI, B. ALBERS; Acoustic Waves in Porous Solid-Fluid Mixtures, in: K. Hutter, N. Kirchner (eds.), *Dynamic Response of Granular and Porous Materials under Large and Catastrophic Deformations*, Springer, Berlin, 285-313, 2002.
- [7] S. FOTI, C. LAI, R. LANCELLOTTA; Porosity of Fluid-saturated Porous Media from Measured Seismic Wave Velocities, *Géotechnique*, **52**, 359-373, 2002.
- [8] C. LAI; *Simultaneous Inversion of Rayleigh Phase Velocity and Attenuation for Near-Surface Site Characterization*, PhD Thesis, Georgia Institute of Technology, Georgia, 1998.
- [9] I. EDELMAN, K. WILMANSKI; Asymptotic analysis of surface waves at vacuum/porous medium and liquid/porous medium interface, *Cont. Mech. Thermodyn.*, **14**, 1, 25-44, 2002.
- [10] S. FOTI; *Multistation Methods for Geotechnical Characterization using Surface Waves*, PhD Thesis, Politecnico di Torino, Turin, 2000.